© 2023. Published by The Company of Biologists Ltd | Journal of Cell Science (2023) 136, jcs261025. doi:10.1242/jcs.261025

PERSPECTIVE

SPECIAL ISSUE: CELL BIOLOGY OF MOTORS

The potential of myosin and actin in nanobiotechnology

Alf Månsson*

ABSTRACT

Since the late 1990s, efforts have been made to utilize cytoskeletal filaments, propelled by molecular motors, for nanobiotechnological applications, for example, in biosensing and parallel computation. This work has led to in-depth insights into the advantages and challenges of such motor-based systems, and has yielded small-scale, proof-of-principle applications but, to date, no commercially viable devices. Additionally, these studies have also elucidated fundamental motor and filament properties, as well as providing other insights obtained from biophysical assays in which molecular motors and other proteins are immobilized on artificial surfaces. In this Perspective, I discuss the progress towards practically viable applications achieved so far using the myosin II–actin motor–filament system. I also highlight several fundamental pieces of insights derived from the studies. Finally, I consider what may be required to achieve real devices in the future or at least to allow future studies with a satisfactory cost–benefit ratio.

KEY WORDS: Molecular motor, Myosin, Actin, Nanotechnology, Lab-on-a chip, Parallel computing

Introduction

Biological molecular motors produce cellular motion and forces leading to muscle contraction, non-muscle cell motility (e.g. cell division and immune cell activity) and intracellular transport of organelles. Molecular motor function also plays roles in diseases, making them interesting drug targets (Trivedi et al., 2020) in conditions such as hypertrophic cardiomyopathy, the leading cause of sudden cardiac death in young people (Maron, 2018; Usaj et al., 2022; Yotti et al., 2019), cancer (Picariello et al., 2019) and diseases caused by apicomplexan parasites such as malaria (Mueller et al., 2017; Trivedi et al., 2020; Vahokoski et al., 2022). Molecular motors are distinguished from other enzymes by being able to utilize the changes in enzyme shape during the turnover of ATP for production of force and motion. For so called linear molecular motors, this is achieved by cyclic affinity changes of the motor to its biological track (a cytoskeletal filament or nucleic acid) coordinated with swings of an integral protein structure acting as a lever arm. The latter amplifies the Ångström-scale structural changes around the active site during the motor-catalyzed turnover of ATP to displacements on a nanometer scale.

The linear molecular motor systems that have primarily been exploited for applications in nanotechnology are actin-based myosin II motors from skeletal muscle and microtubule-based kinesin-1 motors (Reuther et al., 2021a; Saper and Hess, 2020). The efforts towards applications began in the 1990s (Nicolau et al., 1999; Suzuki et al., 1997), stimulated by introduction of the *in vitro* gliding motility assay where cytoskeletal filaments are propelled by surface-immobilized motors (Howard et al., 1989; Kron and Spudich, 1986). Various goals have been pursued, but primarily focusing on (1) lab-on-a chip variants for nanoseparation and biosensing, (2) nano and micro characterization of the topography or materials, and (3) biocomputation. The development in these different areas over time are reviewed in a range of papers covering different time periods (Agarwal and Hess, 2010; Hess, 2011; Korten et al., 2010; Månsson, 2012; Reuther et al., 2021a; Saper and Hess, 2020; van den Heuvel and Dekker, 2007).

Biased by my own work and general research interests, I focus on actin and myosin, using the proteolytic motor fragment heavy meromyosin (HMM) from fast skeletal muscle myosin II family proteins. However, the key prerequisites for exploitation are similar for other motor systems; these include (i) faithful unidirectional guidance of motor propelled filaments along nano and microfabricated paths, (ii) attachment of molecular cargoes, such as antibodies to the filaments, and (iii) extended motility longevity and shelf-life during storage.

Below, I will discuss the basic developments that have enabled the application of myosin motor fragments and consider their contribution to further our understanding of the motor and cytoskeletal filament structure and function. I will also present details for key applications, as well as highlight the remaining challenges that need to be overcome for development of commercially viable devices.

Surface chemistry and spatial selectivity of motor function

For many nanotechnological applications of myosin and actin, limitation of myosin motor functionality to dedicated paths is crucial, for example, to allow the filaments to reliably search a maze of tracks or transport cargoes between well-defined locations. To achieve this can be challenging because, in order to guide actin filaments unidirectionally (without U-turns), it is important to use paths that are narrower than 700 nm and preferentially <300 nm (Sundberg et al., 2006b). This rules out the use of conventional substrates for adsorption of myosin motor fragments, such as nitrocellulose, that is not readily nano-patterned.

Gold tracks for motility, surrounded by protein-repellent polyethyleneglycol (PEG)-silane, have been used for immobilization of kinesin in 1 µm wide channels (van den Heuvel et al., 2005), However, in my experience it is challenging to reproducibly perform all the required nanofabrication steps to achieve nanostructured tracks for high-quality myosin-driven motility this way. Another, somewhat simpler, strategy for selective motility relies on the finding that the actin filament motility quality (the fraction of motile filaments and velocity of the motile filaments) using HMM as the myosin motor fragment is high on moderately hydrophobic surfaces but poor or absent on negatively charged hydrophilic surfaces (Albet-Torres et al., 2007; Balaz et al., 2007; Hanson et al., 2017; Lindberg et al., 2018; Månsson et al., 1989; Nicolau et al., 2007; Persson et al., 2010; Sundberg et al., 2006a, 2003; Suzuki et al., 1997; van Zalinge et al., 2012, 2015). In early studies, we tested a range of flat (not nanopatterned)

Department of Chemistry and Biomedical Science, Linnaeus University, SE-391 82 Kalmar, Sweden.

*Author for correspondence (Alf.mansson@lnu.se)

Journal of Cell Science (2023) 136, jcs261025. doi:10.1242/jcs.261025

monochlorosilane-derivatized glass and SiO_2 surfaces (Albet-Torres et al., 2007; Sundberg et al., 2003). In a systematic study (Albet-Torres et al., 2007), we estimated both hydrophobicity and surface charge, by measuring the contact angle of water droplets (Fig. 1A) and the surface *z*-potential, respectively. We found that motility improved with increased hydrophobicity and became worse with increased negative surface charge; the surface charge and hydrophobicity are inversely related. Nevertheless, studies using positively charged surfaces suggest that the combination of negative charge and moderate hydrophobicity are important because myosin-driven actin filament motility on positively charged surfaces generally exhibits lower velocity (Albet-Torres et al., 2010; Harada et al., 1990; Manandhar et al., 2005).

In our initial study, we performed *in vitro* motility assays using methylcellulose in the solution, which allows motility at a low density of functional motors (Albet-Torres et al., 2007). Using this approach, we found that the velocity increased linearly with the contact angle of the surface starting at a contact angle of ∼30° with no motility at lower contact angles (e.g. as seen on pure SiO_2 and glass) (Fig. 1B). Based on these studies, we arrived at trimethylchlorosilane (TMCS)-derivatized surfaces as optimal for motility, with a contact angle in the range 70–85°. Conversely, negatively charged hydrophilic surfaces (e.g. pure SiO_2/glass or polymers subjected to plasma ashing (e.g. PMMA and CSAR)] are suitable substrates for motility suppressing surfaces. This combination is also readily compatible with standard nanofabrication approaches (Lindberg et al., 2018; Sundberg et al., 2006b) to produce channels with profiles such as those indicated schematically in Fig. 1C. Interestingly, 'standard' nitrocellulose-coated surfaces have a contact angle of 67–76° (Hanson et al., 2017; Nicolau et al., 2007; Sundberg et al., 2003; van Zalinge et al., 2012), which is similar to that of TMCS-derivatized glass or TMCS-derivatized SiO_2. However, as mentioned above, nitrocellulose cannot be nanopatterned.

After establishing TMCS and negatively charged hydrophilic surfaces as optimal for motility-supporting and motility-suppressing areas on nanostructured chips, this strategy (Fig. 1C) has been used in a range of studies (e.g. Lard et al., 2013; Nicolau et al., 2016; Surendiran et al., 2022; Zhu et al., 2022). Further investigations using a range of methods, such as total internal reflection fluorescence (TIRF), fluorescence interference contrast (FLIC) microscopy, quartz crystal microbalance (QCM) and ATPase assays, elucidated the underlying mechanistic basis for the differences in motility quality. These studies (Albet-Torres et al.,

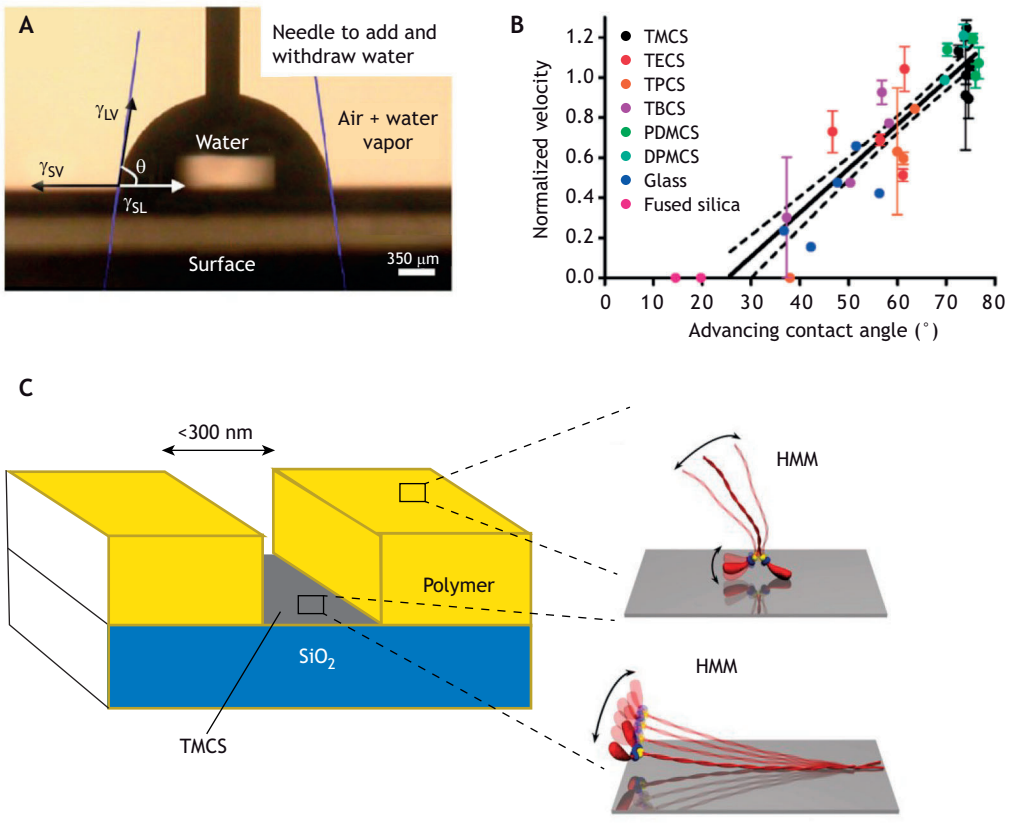

Fig. 1. Adsorption of HMM on differently modified SiO_2 or glass surfaces – foundations for selective motility in nano-channels. (A) Method to assess surface hydrophobicity using contact angle (θ) at the triple point between the gas phase, water droplet and surface. The contact angle is related to surface–liquid (γ_{SL}), surface–vapor (γ_{SV}) and liquid–vapor (γ_{LV}) tensions as: $\gamma_{SV=}\gamma_{SL}+\gamma_{LV}\cos(\theta)$. (B) Mean±s.e.m. velocity (from three surface batches) of HMM-propelled actin filaments in an assay solution with 1 mM MgATP, 130 mM ionic strength and 0.6% methylcellulose, normalized to that on TMCS-derivatized surface. Other surfaces tested in addition to fused silica and glass were derivatized with the monochlorosilanes: triethylchlorosilane (TECS), tripropylchlorosilane (TPCS), tributylchlorosilane (TBCS), phenyldimethylchlorosilane (PDMCS) and diphenylmethylchlorosilane (DPMCS). (C) Schematic of nanoscale channel with TMCS-derivatized SiO_2 floor and with walls and surrounding areas made up of hydrophilic negatively charged polymer. The expansions on the right show models (Persson et al., 2010) for major HMM configuration on TMCS-derivatized and negatively charged hydrophilic surfaces based on results in Albet-Torres et al. (2007), Balaz et al. (2007), Månsson et al., (2008), Persson et al. (2010) and Sundberg et al. (2006a). Panel A modified from Månsson, 2012 where it was published under a CC-BY 2.0 licence. Panel B reprinted with permission from Albet-Torres et al. (2007) and insets in panel C reprinted with permission from Persson et al. (2010). Copyright 2007 and 2010, American Chemical Society.

Journal of Cell Science (2023) 136, jcs261025. doi:10.1242/jcs.261025

2007; Balaz et al., 2007; Persson et al., 2010; Sundberg et al., 2006a) led to models for the adsorption of HMM to TMCS, on the one hand, and a negatively charged hydrophilic surface, on the other hand (insets in Fig. 1C). An interesting finding was a consistently higher amplitude of a slow phase of ATP turnover (10–100-fold lower than basal myosin ATPase in solution) for HMM molecules adsorbed to a negatively charge surfaces (Persson et al., 2010). Most likely, this low ATP turnover rate is associated with the slowing of essential inter-domain movements in the surface-immobilized myosin head during ATP turnover, consistent with similar slowing when myosin heads are 'parked' on the thick filament backbone in muscle in the so called inter-acting head motif, which corresponds to the super-relaxed state (McNamara et al., 2015; Nag and Trivedi, 2021; Stewart et al., 2010; Toepfer et al., 2020).

Guiding along channels

As noted above, selective motility on the floors of TMCS-derivatized nanochannels, without any motility on the surrounding negatively charged polymer layers, is one important prerequisite for guiding motor-propelled actin filaments with minimal risk for filament escape. However, this is not sufficient to confine the filaments to the tracks. Addition of topographical barriers, to form nano-channels (Fig. 1C), is also essential, particularly to prevent filament escape at corners and junctions owing to the rather high actin filament bending stiffness (flexural rigidity) with a persistence length of 10–20 µm (Gittes et al., 1993; Isambert et al., 1995; Vikhorev et al., 2008). The filament persistence length (L_P) is directly proportional to the flexural rigidity, EI where E is the Young's modulus and I is the second moment of inertia of the filament cross-section. Thus, $L_P=EI/k_BT$, relates the flexural rigidity to thermal energy (k_BT; Bolzmann constant multiplied by absolute temperature), consistent with L_P representing a correlation distance along a filament under thermal fluctuations, over which 'memory' of the tangent angle a given distance from the starting point is lost.

The persistence length also governs the maximum allowed channel width that ensures unidirectional transport of filaments without U-turns. Owing to the ∼10-fold lower persistence length of individual actin filaments compared to microtubules propelled by kinesin-1 (Nitta et al., 2008), narrower channel widths are critical. Specifically, a channel width of <300 nm is required for 100% unidirectional transport, with a width below 900 nm yielding a satisfactory level (1 mm gliding with only 10% U-turns) with HMM-propelled actin filaments. In contrast, a channel width of up to 19 µm is sufficient for satisfactory unidirectional transport in case of kinesin-1-propelled microtubules. The lower persistence length of actin filaments also makes these more prone to turn 90° at channel junctions compared to kinesin-propelled microtubules. This is reflected in larger error rates when these different motor–filament systems are compared when used in network-based biocomputation (Nicolau et al., 2016; Surendiran et al., 2022). The importance of the filament persistence length for such applications has prompted detailed studies (Bengtsson et al., 2016; Ishigure and Nitta, 2015; Lard et al., 2013; Månsson et al., 2012; Nitta and Hess, 2005; Nitta et al., 2008; Vikhorev et al., 2008). These have demonstrated, as predicted from theoretical work (Duke et al., 1995), that the persistence length of actin filaments can be approximately estimated from the statistics of the sliding paths in *in vitro* motility assays, albeit with some complexities. It is of interest to note that increased persistence length can be achieved for HMM-propelled bundles of actin filaments that are cross-linked by fascin (Takatsuki et al., 2014).

Another functional characteristic that is important for filament guiding along nanochannels is the degree of motor processivity. Processivity refers to the tendency for an individual motor to take several steps along its track before detaching. Highly processive motors such as myosin V can move more than 1 µm along an actin filament, corresponding to >27 steps of the two-headed motor (Sakamoto et al., 2003), before diffusing away from the filament. In contrast, non-processive motors such as fast skeletal muscle myosin II just takes one step before detaching. Therefore, myosin II motors must work in teams to effectively propel actin filaments.

In applications where motor-driven filaments are guided along nanochannels, high processivity increases the tendency for the motor-propelled filaments to climb up the wall and escape into solution. With high processivity, the risk also increases that filaments can enter directly into a channel from solution rather than being transported with the desired directionality into the channels from a dedicated filament loading zone (Fig. 2). The reason is that as little as a single unblocked processive motor (outside dedicated tracks) is sufficient to capture a filament and propel it. Moreover, filaments propelled by motors with a low degree of processivity might risk detachment from the track if the motor density is low somewhere in the channel, because there might not be a sufficient number of motors for them to remain attached to the filament at all times.

Cargo transportation

Cargoes (e.g. organelles, vesicles) that are transported in cells are typically attached to processive molecular motors while they move along cytoskeletal filaments (Ross et al., 2008). Cargo transportation in nanotechnological applications do not directly mimic the cellular strategy. Instead, the cargo is normally attached to the filaments that are then propelled by surface adsorbed motors. The reason is that it is somewhat more straightforward to generate predetermined cargo transportation routes on a chip by selective motor adsorption in nanoscale channels than laying down well-controlled cytoskeletal networks *in vitro*, although attempts have been made at the latter (e.g. Huang et al., 2006).

A range of approaches exist, from various forms of covalent functionalization of actin filaments with different cargoes, via lysine residues or Cys374, to the use of natural actin-binding peptides, such as phalloidin, as 'handles' for cargo attachment. The underlying chemistry and the avoidance of issues such as actin filament cross-linking are reviewed elsewhere (Kumar and Månsson, 2017). However, there are also important considerations with regard to motor–filament biology. First, any chemical modification must not destabilize the filaments or compromise the ability of actin to polymerize, which might occur when some (but not all) types of molecular cargo are immobilized to actin via Cys374, as this could interfere with a hydrophobic cleft in subdomain 1 of actin (Kumar and Månsson, 2017; Murakami et al., 2010), which is important for the longitudinal strength of the filament. Generally, cargo attachment to actin via lysine residues appears to have less functional consequences. A second aspect to consider is to avoid inhibition of myosin-propelled motility owing to cargo presence, an effect that is reduced with reduced cargo size (Persson et al., 2013). Indeed, several small molecular cargo molecules (e.g. biotin) can be attached to each actin subunit (>1000 per µm) without any appreciable motility inhibition, whereas for protein cargoes (antibody–antigen complexes or streptavidin), only a maximum of ∼20% of the actin subunits (<70 per µm of the filament) can be loaded with cargo before there is an appreciable reduction in velocity and even greater reduction in the fraction of motile filaments (Persson et al., 2013)

Motility inhibition becomes more severe with further increase in cargo size as demonstrated for 20 nm nanoparticles and lipid

Journal of Cell Science (2023) 136, jcs261025. doi:10.1242/jcs.261025

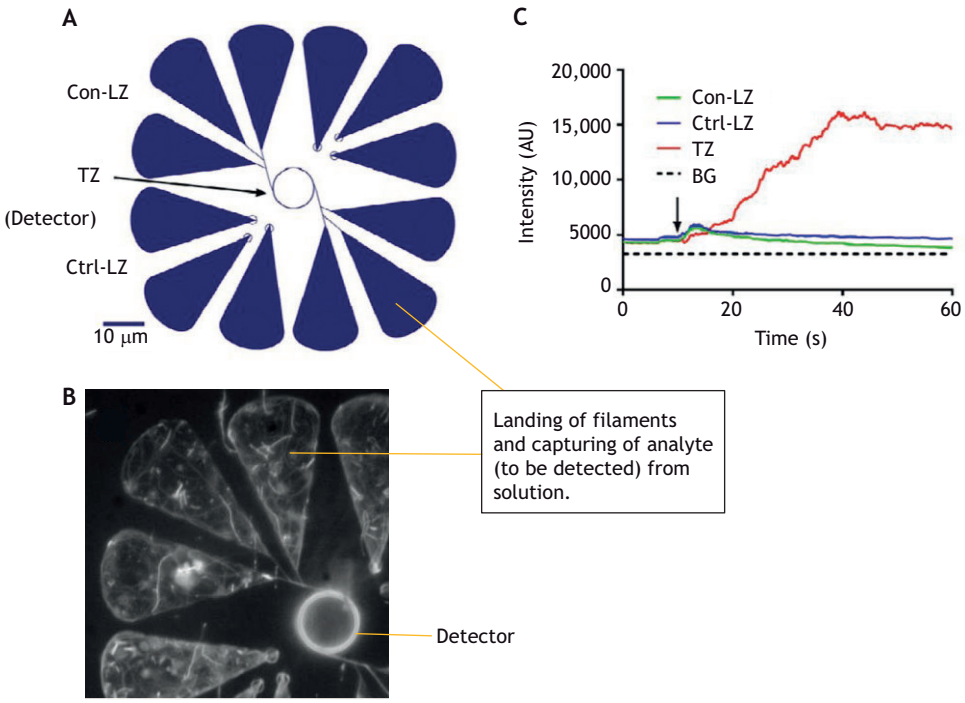

Fig. 2. Proof-of-principle concentration and detection device. (A) Design with loading zones (LZ) where filaments land from solution and where any analyte to be detected is intended to be captured on the filaments. The filaments are then intended to be propelled by HMM (active on blue areas only; compare with Fig. 1) to a trapping zone (TZ) corresponding to a detector area in a biosensing device where the filaments (and any captured cargo or analyte) are concentrated. Loading zones are separated into connected loading zones (Con-LZ) and control loading zones (Ctrl-LZ) to facilitate analysis in proof-of-principle device. (B) Operation principle of device illustrated by HMM propulsion of Rhodamine–phalloidin-labelled filaments without analytes. An overlay (*z*-projection of the standard deviation) of the first 600 frames (120 s) illustrates how the filaments are propelled from the loading zones into the trapping zone (corresponding to the detector area) where they are concentrated. (C) Time courses of average fluorescence intensities integrated over the trapping zone, Con-LZ and Ctrl-LZ. Note, appreciably higher intensity in trapping zone than in the loading zones as evidence for the concentration of filaments. Arrow, ATP infusion. Note, there is a further smaller decrease in fluorescence intensity in Ctrl-LZ (due to photobleaching) compared to that in Con-LZ (due to photobleaching and transport of filaments into TZ). AU, arbitrary units. Figure modified from Lard et al. (2013) with permission from Elsevier.

vesicles of >50 nm diameter (Persson et al., 2013). Further studies are required to fully understand the mechanisms underlying motility inhibition, but likely factors include interactions between the cargoes and the underlying surface, as well as the cargo-blocking myosin-binding sites on actin. This would inhibit the sequential action of the two heads of each HMM molecule, or slippage of myosin heads between neighboring actin sites as has been suggested in some models (Caremani et al., 2013; Esaki et al., 2007; Marcucci and Yanagida, 2012).

Inhibition of motility owing to blockage of myosin-binding sites along the actin filament is consistent with an increased cargo-carrying capacity (per bundle length but not per number of actin subunits) when the cargoes are attached to actin filaments bundled via fascin (Kumar et al., 2016). Such bundles might thus be useful to expand the cargo capacity of actin filaments. In addition, other developments including methods for programmed cargo pick-up and release at predetermined positions would be of value. Of particular interest here is the transport of oligonucleotides attached to actin filaments, as these are readily programmable handles for a range of secondary cargoes as recently demonstrated for the microtubule–kinesin system (Keya et al., 2018). However, myosin-driven transport of actin filaments with oligonucleotide cargoes is yet to be demonstrated.

Longevity and shelf-life

For possible real-world applications, for instance in medical diagnostics (see below), the shelf-life of the entire device and its protein components are important, as the devices need to be stored under easily achievable conditions between their manufacturing and use. It is therefore important that it has been shown that *in vitro* motility assay flow cells, with HMM adsorbed to TMCS surfaces, can be stored in appropriate salt solutions at 4°C for up to 2 weeks with only limited deterioration of function (Albet-Torres and Månsson, 2011; Sundberg et al., 2003) and for more than a month (in assay solution) at −20°C, such as in an ordinary household freezer (Albet-Torres and Månsson, 2011). Moreover, the isolated proteins (HMM and F-actin) can be stored at −80°C for years, before being incorporated into a device (Balaz and Månsson, 2005; Salhotra et al., 2021).

In addition, the operation duration of the actual nanodevice is of importance for some applications. For instance, diagnostics applications are likely to require some time for capturing and transporting analytes to a detector surface and, in order to ensure robustness of the system, the life-time of the device should be longer than required for the analysis itself. Moreover, in biocomputation, this would be especially valuable with hours to days of experimentation required in order to increase the effective total number of filaments, thereby allowing researchers to overcome computational errors. Prolonged experimentation would actually contribute to achieving this through the recycling of filaments, something that has already been implemented in biocomputation networks (Nicolau et al., 2016; Zhu et al., 2022) (van Delft et al., 2022).

Several factors are important for a prolonged function of surface-immobilized motors, both in a typical *in vitro* motility assay, and in motor-driven nanodevices. In addition to the obvious importance of

Journal of Cell Science (2023) 136, jcs261025. doi:10.1242/jcs.261025

avoiding any toxic components during the production of flow cells or nanostructured surfaces, other factors to consider include prevention of (1) oxygen access to the flow cell (of particular importance), (2) drying out of the flow cell, (3) HMM surface denaturation, (4) HMM surface desorption, (5) actin filament detachment, and (6) accumulation of products of ATP turnover, as discussed in detail elsewhere (Reuther et al., 2021a; Salhotra et al., 2021).

Types of myosin–actin-based devices and associated challenges

The development of molecular motor-based devices was partly motivated by the cellular tasks performed by the motors. Of particular interest here is the transport of cargoes that has the potential to produce lab-on-a-chip applications with a greater degree of miniaturization and other potential advantages compared to traditional systems. For instance, systems that rely on microfluidics for transport depend on accessory infrastructure such as pumps that can have substantial complexity and bulkiness (Jokerst et al., 2010; Whitesides, 2006). Moreover, if nanofluidics is to be used for transport of molecules in solution, strong driving forces are required (Månsson et al., 2005). These challenges can be overcome by using molecular-motor-driven filaments to transport cargoes or particles. The movement of motor-driven filaments with attached cargoes requires only low energy input, achieved by supplying an ATP-containing solution. Proof-of-principle motor-driven lab-on-a-chip devices include biosensing chips for diagnostics and nanoseparation, in which recognition elements, for example, antibodies, are immobilized on the actin filaments (Kumar et al., 2016, 2012, 2013; Lard et al., 2013). Such devices can be used to capture analyte molecules from a large fluid volume by searching over large surface areas (Katira and Hess, 2010; Lard et al., 2013) as exemplified by the loading zones shown in Fig. 2. Most simplistically, the analyte molecule can then be detected by observing its movement together with the filaments (e.g. via fluorescent antibodies in sandwich configuration) or an aggregation of motile filaments owing to antibody–analyte crosslinks (Reuther et al., 2021a).

After they have captured analytes, the filaments can be concentrated on a nanoscale detector area (Lard et al., 2013) (see Fig. 2 for such a device). Here, an increased fluorescence intensity is detected in a central circular area into which filaments are transported from larger surrounding loading zones. In the same work, a more realistic (but less visually clear) concentration of molecules into a central detector area could be demonstrated for fluorescence-labelled streptavidin captured by biotinylated filaments (Lard et al., 2013).

In subsequent studies, we achieved a higher capacity (per length) to transport antibodies and their captured antigen by immobilizing antigens on actin filament bundles generated by fascin crosslinking, which allowed us to demonstrate two modes of detection, that is, transport of the fluorescent antigen attached to the bundles or formation of bundle aggregates (Fig. 3).

To summarize the above, we have demonstrated that we can achieve getting an effective concentration of analyte (e.g. antigen) into a detector area and are able to overcome issues related to shelf-life (months at −20°C; years at −80°C) and operational longevity (hours up to a day). However, a key remaining challenge is the inhibition of myosin-driven actin filament motility (as well as kinesin-driven microtubule motility) in body fluids such as blood plasma (Korten et al., 2013).

Another application that has been recently addressed by using myosin-driven actin filaments moving in nano-networks is the solution of so called non-deterministic polynomial (NP) complete combinatorial problems. These problems explode in computation time (and associated energy requirements) using conventional electronic (serial) computers when the problem size increases. Examples of problems of this type are prediction of protein folding and network routing (selecting paths that are optimal in several

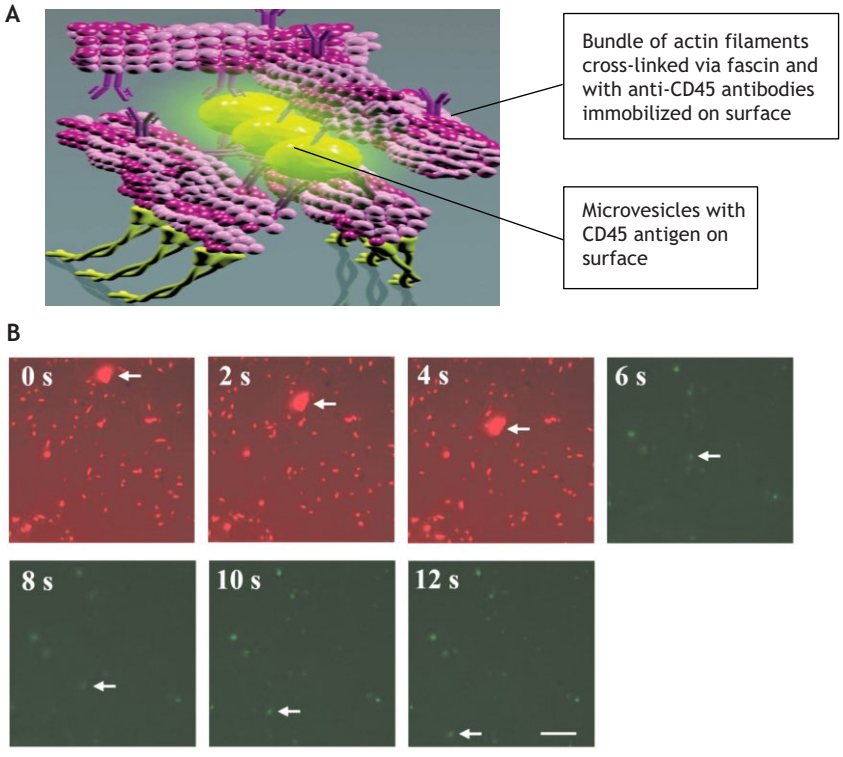

Fig. 3. Transportation of leukaemia-specific microvesicles attached to specific monoclonal anti-CD45 antibodies immobilized on the surface of fascin-bundled actin filaments. (A) Schematic illustration of three microvesicles (green) attached to, and aggregating, four different actin filament bundles, via specific antibodies on the bundles. (B) Time series of fluorescence micrographs illustrating HMM-driven transport of fascin–actin bundles aggregated via microvesicle(s) (arrow) as illustrated schematically in A. The actin filament bundle was labelled by Rhodamine–phalloidin (red) and the microvesicle(s) by the cytoplasmic dye CFSE (green fluorescence). The microvesicle(s) were attached to the bundles via specific antibodies as in A. In time frames 0–4 s, the fluorescence microscope filter set was set to allow visualization of actin fluorescence whereas in time frames 6–12 s the filter set was changed to observe the microvesicle fluorescence. Figure modified from Kumar et al. (2016) with permission from the Royal Society of Chemistry.

Journal of Cell Science (2023) 136, jcs261025. doi:10.1242/jcs.261025

respects through complex networks). It is therefore of interest to explore alternative approaches, and one of those is the so-called network-based biocomputation (NBC). Here, a large number of biological agents, for example, actin filaments propelled by myosin motor fragments, explore networks of nanofabricated channels, whereby the network geometry encodes the problem (depicted in Fig. 4). Thus far, we have demonstrated in proof-of-principle experiments that motor-propelled filaments can solve a wide range of such problems albeit of rather small size (e.g. Nicolau et al., 2016; van Delft et al., 2022). Up-scaling efforts are currently ongoing by using strategies that include expansion of network size, increased filament number, more efficient encoding algorithms and tagging of the filaments for posterior identification of their path through the network. Tags in this context could be an array of fluorescent objects where the combination of colours produce a barcode, or DNA oligonucleotides where different DNA sequences would be unique barcodes. Despite having only been researched for 10 years and with funding several-fold lower than for instance for quantum computation, notable progress has been made (van Delft et al., 2022). However, there are a number of remaining key challenges that include the effective capturing, transport and read-out of a large number of tagging elements (e.g. DNA) on each filament, as well as minimization of traffic rule errors, for example, filaments taking non-allowed turns at network junctions. The latter problem can be appreciably reduced by using an optimized network geometry as well as increasing persistence length of the filaments. This could be achieved with the use of fascin-bundled filaments instead of individual actin filaments. Moreover, traffic rule errors could be completely overcome with the use of crossings in the 3D plane, as has been demonstrated in proof-of-principle experiments for kinesin-propelled microtubules (Reuther et al., 2021b).

In addition to lab-on-a-chip applications and NBC, a range of other applications have been considered, including material characterization, such as demonstration of light-guiding of semiconductor nanowires (Ten Siethoff et al., 2014), a phenomenon that, together with other findings formed the basis for a patent and a company in diagnostics (https://alignedbio.com/). Moreover, myosin-driven actin filaments might also be used for surface chemistry characterization on the nanoscale, based on their sensitivity to small changes in the surface contact angle on negatively charged surfaces. For more details on these and other specialized applications, see recent reviews (Reuther et al., 2021a; Saper and Hess, 2020).

Perspectives and conclusions

The field exploring biological molecular motors in technology has, as was predicted in a review more than 15 years ago (van den Heuvel and Dekker, 2007), continued to be an interdisciplinary playground leading to new fundamental insights into protein biophysics, materials properties and protein–surface interactions as well as leading to conceptually new solutions in biosensing, diagnostics and parallel computation. However, the developments thus far have been largely on the small scale and exploratory, and although some patents have been filed (e.g. Månsson and Tågerud, 2014), there are not any large scale industrial or health-care applications to date.

The field is likely to continue as an interdisciplinary endeavour that will contribute new knowledge to different disciplines.

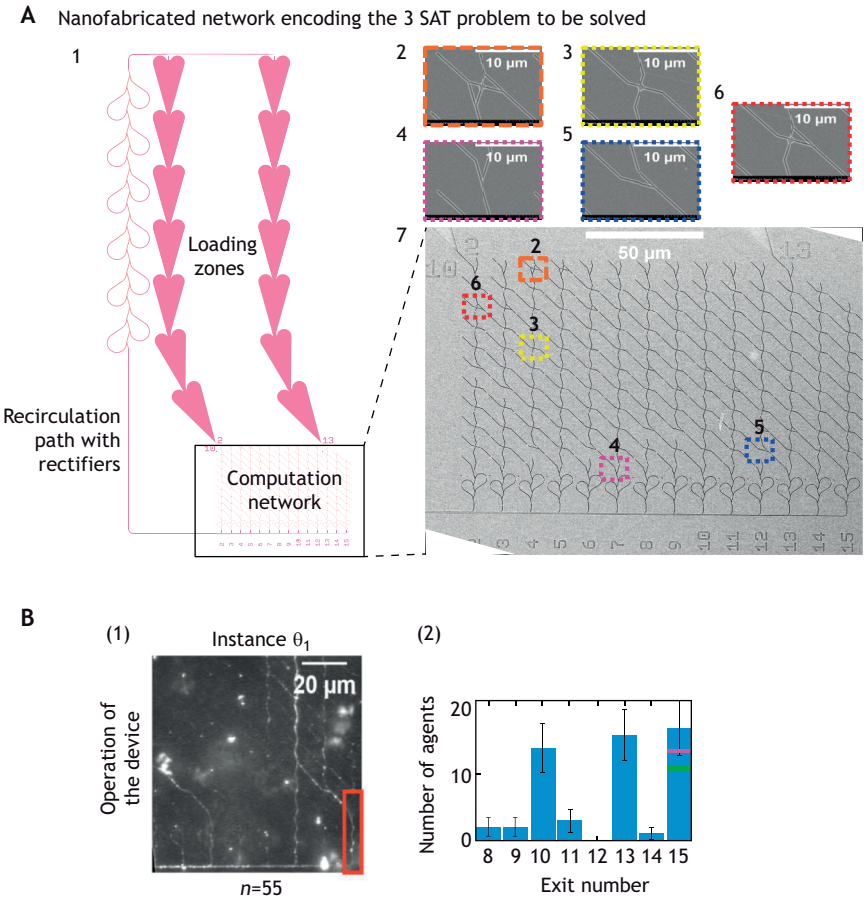

Fig. 4. Solving a small instance of a 3-SAT NP complete problem using network-based biocomputation. (A) (1) Schematic device layout. 3-SAT, satisfiability. Filaments enter the network via the loading zones at two entrances on the top and exit the network at the bottom. They are then recycled via the recirculation path and guided back to loading zones re-use in the computation. (2) Scanning electron microscopy (SEM) image of an important architectural element in the device, a so-called split junction. (3) SEM image of a pass junction. (4) SEM image of a reset-FALSE junction. (5) SEM image of a reset-TRUE junction. (6) SEM image of a split top junction. (7) SEM image of the overall network. (B) Experimental read-out for the problem instance encoded by network in A. (1) Standard deviation of intensity values among 1000 typical fluorescence micrographs (400 s) of actin filaments moving through the device, indicating the most used paths. (2) Experimental results obtained from manually counted actin filaments passing the exits at the bottom. Total counted events (n) given with error bars representing counting errors, $\sqrt{n}$. For the target column corresponding to satisfiability for the specific problem, (15 in red boxes in 1), values above the magenta bar are significantly correct (P<0.01, corresponding to 99% confidence level whereas values below the green bar are significantly incorrect (P<0.01). For details see Zhu et al., (2022), where the figure was published under a CC-BY 4.0 license.

However, future developments towards commercially viable devices will rely on gaining credibility in the biosensing, diagnostics and computation communities to open them to motor-driven devices. This, in turn, requires the demonstration of features that cannot readily be achieved using the conventional systems in use today. In this context, the potential advantages of motor-driven devices are their cheap components with their prolonged shelf-life and longevity, as well as recycling possibilities (Rahman et al., 2019). Moreover, a system with self-propulsion without the need for pumps to drive liquid flow has important advantages, including low energy consumption. The latter is particularly important if other obstacles to the realization of large-scale computation systems can be overcome. However, in order to achieve that, it will be important to not only solve the specific challenges but also to enable industrially standardized production of all device components, from nanofabrication over tagging elements (e.g. DNA) to the motor proteins (details in Reuther et al., 2021a). In contrast, all developments achieved thus far have relied on work in small-scale research groups without any industrialized standardization. This is probably the major 'catch 22' of the field. In order to attract appreciable investments to make it possible to demonstrate the reliable use of motor-driven devices with clear benefits, considerable investments beyond small-scale research projects are required.

Acknowledgements
Dr Till Korten at the Technical University of Dresden is acknowledged for providing original figures as a basis for the present Fig. 4.

Competing interests
A.M. has applied for patents in this field (although not all of these are currently active), and also has some shares in Aligned bio (https://alignedbio.com/), which works on advanced nanowire sensor platforms and film technologies.

Funding
My work in this area is supported by the European Union [228971 (MONAD), 613044 (ABACUS), 732482 (Bio4comp)] and the Swedish Research Council (2015-05290, 2019-03456).

References
Agarwal, A. and Hess, H. (2010). Biomolecular motors at the intersection of nanotechnology and polymer science. *Prog. Polym. Sci.* **35**, 252-277. doi:10.1016/j.progpolymsci.2009.10.007
Albet-Torres, N. and Månsson, A. (2011). Long-term storage of surface-adsorbed protein machines. *Langmuir* **27**, 7108-7112. doi:10.1021/la201081w
Albet-Torres, N., O'Mahony, J., Charlton, C., Balaz, M., Lisboa, P., Aastrup, T., Månsson, A. and Nicholls, I. A. (2007). Mode of heavy meromyosin adsorption and motor function correlated with surface hydrophobicity and charge. *Langmuir* **23**, 11147-11156. doi:10.1021/la7008682
Albet-Torres, N., Gunnarsson, A., Persson, M., Balaz, M., Höök, F. and Månsson, A. (2010). Molecular motors on lipid bilayers and silicon dioxide: different driving forces for adsorption. *Soft Mat.* **6**, 3211-3219. doi:10.1039/C0SM00019A
Balaz, M. and Månsson, A. (2005). Detection of small differences in actomyosin function using actin labeled with different phalloidin conjugates. *Anal. Biochem.* **338**, 224-236. doi:10.1016/j.ab.2004.12.012
Balaz, M., Sundberg, M., Persson, M., Kvassman, J. and Månsson, A. (2007). Effects of surface adsorption on catalytic activity of heavy meromyosin studied using fluorescent ATP analogue. *Biochemistry* **46**, 7233-7251. doi:10.1021/bi700211u
Bengtsson, E., Persson, M., Rahman, M. A., Kumar, S., Takatsuki, H. and Månsson, A. (2016). Myosin-induced gliding patterns at varied [MgATP] unveil a dynamic actin filament. *Biophys. J.* **111**, 1465-1477. doi:10.1016/j.bpj.2016.08.025
Caremani, M., Melli, L., Dolfi, M., Lombardi, V. and Linari, M. (2013). The working stroke of the myosin II motor in muscle is not tightly coupled to release of orthophosphate from its active site. *J. Physiol.* **591**, 5187-5205. doi:10.1113/jphysiol.2013.257410
Duke, T., Holy, T. E. and Leibler, S. (1995). "Gliding assays" for motor proteins - a theoretical-analysis. *Phys. Rev. Lett.* **74**, 330-333. doi:10.1103/PhysRevLett.74.330
Esaki, S., Ishii, Y., Nishikawa, M. and Yanagida, T. (2007). Cooperative actions between myosin heads bring effective functions. *Biosystems* **88**, 293-300. doi:10.1016/j.biosystems.2006.03.013
Gittes, F., Mickey, B., Nettleton, J. and Howard, J. (1993). Flexural rigidity of microtubules and actin-filaments measured from thermal fluctuations in shape. *J. Cell Biol.* **120**, 923-934. doi:10.1083/jcb.120.4.923
Hanson, K. L., Fulga, F., Dobroiu, S., Solana, G., Kaspar, O., Tokarova, V. and Nicolau, D. V. (2017). Polymer surface properties control the function of heavy meromyosin in dynamic nanodevices. *Biosens. Bioelectron.* **93**, 305-314. doi:10.1016/j.bios.2016.08.061
Harada, Y., Sakurada, K., Aoki, T., Thomas, D. D. and Yanagida, T. (1990). Mechanochemical coupling in actomyosin energy transduction studied by in vitro movement assay. *J. Mol. Biol.* **216**, 49-68. doi:10.1016/S0022-2836(05)80060-9
Hess, H. (2011). Engineering applications of biomolecular motors. *Annu. Rev. Biomed. Eng.* **13**, 429-450. doi:10.1146/annurev-bioeng-071910-124644
Howard, J., Hudspeth, A. J. and Vale, R. D. (1989). Movement of microtubules by single kinesin molecules. *Nature* **342**, 154-158. doi:10.1038/342154a0
Huang, L., Manandhar, P., Byun, K. E., Chase, P. B. and Hong, S. (2006). Selective assembly and alignment of actin filaments with desired polarity on solid substrates. *Langmuir* **22**, 8635-8638. doi:10.1021/la061008a
Isambert, H., Venier, P., Maggs, A. C., Fattoum, A., Kassab, R., Pantaloni, D. and Carlier, M. F. (1995). Flexibility of actin filaments derived from thermal fluctuations. Effect of bound nucleotide, phalloidin, and muscle regulatory proteins. *J. Biol. Chem.* **270**, 11437-11444. doi:10.1074/jbc.270.19.11437
Ishigure, Y. and Nitta, T. (2015). Simulating an actomyosin in vitro motility assay: toward the rational design of actomyosin-based microtransporters. *IEEE Trans. Nanobioscience* **14**, 641-648. doi:10.1109/TNB.2015.2443373
Jokerst, J. V., Jacobson, J. W., Bhagwandin, B. D., Floriano, P. N., Christodoulides, N. and Mcdevitt, J. T. (2010). Programmable nano-bio-chip sensors: analytical meets clinical. *Anal. Chem.* **82**, 1571-1579. doi:10.1021/ac901743u
Katira, P. and Hess, H. (2010). Two-stage capture employing active transport enables sensitive and fast biosensors. *Nano Lett.* **10**, 567-572. doi:10.1021/nl903468p
Keya, J. J., Suzuki, R., Kabir, A. M. R., Inoue, D., Asanuma, H., Sada, K., Hess, H., Kuzuya, A. and Kakugo, A. (2018). DNA-assisted swarm control in a biomolecular motor system. *Nat. Commun.* **9**, 453. doi:10.1038/s41467-017-02778-5
Korten, T., Månsson, A. and Diez, S. (2010). Towards the application of cytoskeletal motor proteins in molecular detection and diagnostic devices. *Curr. Opin. Biotechnol.* **21**, 477-488. doi:10.1016/j.copbio.2010.05.001
Korten, S., Albet-Torres, N., Paderi, F., Ten Siethoff, L., Diez, S., Korten, T., Te Kronnie, G. and Månsson, A. (2013). Sample solution constraints on motor-driven diagnostic nanodevices. *Lab. Chip* **13**, 866-876. doi:10.1039/c2lc41099k
Kron, S. J. and Spudich, J. A. (1986). Fluorescent actin-filaments move on myosin fixed to a glass-surface. *Proc. Natl. Acad. Sci. USA* **83**, 6272-6276. doi:10.1073/pnas.83.17.6272
Kumar, S. and Månsson, A. (2017). Covalent and non-covalent chemical engineering of actin for biotechnological applications. *Biotechnol. Adv.* **35**, 867-888. doi:10.1016/j.biotechadv.2017.08.002
Kumar, S., Ten Siethoff, L., Persson, M., Lard, M., Te Kronnie, G., Linke, H. and Månsson, A. (2012). Antibodies covalently immobilized on actin filaments for fast myosin driven analyte transport. *PLoS One* **7**, e46298. doi:10.1371/journal.pone.0046298
Kumar, S., Tensiethoff, L. and Månsson, A. (2013). Magnetic separation alleviates deleterious effects of blood serum on actomyosin based diagnostics device. *J. Nanobiotechnol.* **11**, 14.
Kumar, S., Milani, G., Takatsuki, H., Lana, T., Persson, M., Frasson, C., Te Kronnie, G. and Månsson, A. (2016). Sensing protein antigen and microvesicle analytes using high-capacity biopolymer nano-carriers. *Analyst* **141**, 836-846. doi:10.1039/C5AN02377G
Lard, M., Ten Siethoff, L., Kumar, S., Persson, M., Te Kronnie, G., Linke, H. and Månsson, A. (2013). Ultrafast molecular motor driven nanoseparation and biosensing. *Biosens. Bioelectron.* **48**, 145-152. doi:10.1016/j.bios.2013.03.071
Lindberg, F. W., Norrby, M., Rahman, M. A., Salhotra, A., Takatsuki, H., Jeppesen, S., Linke, H. and Månsson, A. (2018). Controlled surface silanization for actin-myosin based nanodevices and biocompatibility of new polymer resists. *Langmuir* **34**, 8777-8784. doi:10.1021/acs.langmuir.8b01415
Manandhar, P., Huang, L., Grubich, J. R., Hutchinson, J. W., Chase, P. B. and Hong, S. H. (2005). Highly selective directed assembly of functional actomyosin on Au surfaces. *Langmuir* **21**, 3213-3216. doi:10.1021/la047227i
Månsson, A. (2012). Translational actomyosin research: fundamental insights and applications hand in hand. *J. Muscle Res. Cell Motil.* **33**, 219-233. doi:10.1007/s10974-012-9298-5
Månsson, A. and Tågerud, S. (2014). Detection Conjugate. *US patent* US 8,658,381. https://image-ppubs.uspto.gov/dirsearch-public/print/downloadPdf/8658381
Månsson, A., Morner, J. and Edman, K. A. (1989). Effects of amrinone on twitch, tetanus and shortening kinetics in mammalian skeletal muscle. *Acta Physiol. Scand.* **136**, 37-45. doi:10.1111/j.1748-1716.1989.tb08627.x

Månsson, A., Sundberg, M., Bunk, R., Balaz, M., Nicholls, I. A., Omling, P., Tegenfeldt, J. O., Tågerud, S. and Montelius, L. (2005). Actin-based molecular motors for cargo transportation in nanotechnology - potentials and challenges. *IEEE Trans. Adv. Pack.* **28**, 547-555. doi:10.1109/TADVP.2005.858309

Månsson, A., Balaz, M., Albet-Torres, N. and Rosengren, K. J. (2008). In vitro assays of molecular motors–impact of motor-surface interactions. *Front. Biosci.* **13**, 5732-5754. doi:10.2741/3112

Månsson, A., Bunk, R., Sundberg, M. and Montelius, L. (2012). Self-organization of motor propelled cytoskeletal filaments at topographically defined borders. *J. Biomed. Biotechnol.* **2012**, 647265. doi:10.1155/2012/647265

Marcucci, L. and Yanagida, T. (2012). From single molecule fluctuations to muscle contraction: a Brownian model of A.F. Huxley's hypotheses. *PLoS One* **7**, e40042. doi:10.1371/journal.pone.0040042

Maron, B. J. (2018). Clinical course and management of hypertrophic cardiomyopathy. *N. Engl. J. Med.* **379**, 655-668. doi:10.1056/NEJMra1710575

Mcnamara, J. W., Li, A., Dos Remedios, C. G. and Cooke, R. (2015). The role of super-relaxed myosin in skeletal and cardiac muscle. *Biophys. Rev.* **7**, 5-14. doi:10.1007/s12551-014-0151-5

Mueller, C., Graindorge, A. and Soldati-Favre, D. (2017). Functions of myosin motors tailored for parasitism. *Curr. Opin. Microbiol.* **40**, 113-122. doi:10.1016/j.mib.2017.11.003

Murakami, K., Yasunaga, T., Noguchi, T. Q. P., Gomibuchi, Y., Ngo, K. X., Uyeda, T. Q. P. and Wakabayashi, T. (2010). Structural basis for actin assembly, activation of ATP hydrolysis, and delayed phosphate release. *Cell* **143**, 275-287. doi:10.1016/j.cell.2010.09.034

Nag, S. and Trivedi, D. V. (2021). To lie or not to lie: Super-relaxing with myosins. *Elife* **10**, e63703. doi:10.7554/eLife.63703

Nicolau, D. V., Suzuki, H., Mashiko, S., Taguchi, T. and Yoshikawa, S. (1999). Actin motion on microlithographically functionalized myosin surfaces and tracks. *Biophys. J.* **77**, 1126-1134. doi:10.1016/S0006-3495(99)76963-8

Nicolau, D. V., Solana, G., Kekic, M., Fulga, F., Mahanivong, C., Wright, J. and Dos Remedios, C. (2007). Surface hydrophobicity modulates the operation of actomyosin-based dynamic nanodevices. *Langmuir* **23**, 10846-10854. doi:10.1021/la700412m

Nicolau, D. V., Jr., Lard, M., Korten, T., Van Delft, F. C., Persson, M., Bengtsson, E., Månsson, A., Diez, S., Linke, H. and Nicolau, D. V. (2016). Parallel computation with molecular-motor-propelled agents in nanofabricated networks. *Proc. Natl. Acad. Sci. USA* **113**, 2591-2596. doi:10.1073/pnas.1510825113

Nitta, T. and Hess, H. (2005). Dispersion in active transport by kinesin-powered molecular shuttles. *Nano Lett.* **5**, 1337-1342. doi:10.1021/nl050586t

Nitta, T., Tanahashi, A., Obara, Y., Hirano, M., Razumova, M., Regnier, M. and Hess, H. (2008). Comparing guiding track requirements for myosin- and kinesin-powered molecular shuttles. *Nano Lett.* **8**, 2305-2309. doi:10.1021/nl8010885

Persson, M., Albet-Torres, N., Sundberg, M., Ionov, L., Diez, S., Höök, F., Månsson, A. and Balaz, M. (2010). Heavy meromyosin molecules extend more than 50 nm above adsorbing electronegative surfaces. *Langmuir* **26**, 9927-9936. doi:10.1021/la100395a

Persson, M., Gullberg, M., Tolf, C., Lindberg, A. M., Månsson, A. and Kocer, A. (2013). Transportation of nanoscale cargoes by Myosin propelled actin filaments. *PLoS One* **8**, e55931. doi:10.1371/journal.pone.0055931

Picariello, H. S., Kenchappa, R. S., Rai, V., Crish, J. F., Dovas, A., Pogoda, K., Mcmahon, M., Bell, E. S., Chandrasekharan, U., Luu, A. et al. (2019). Myosin IIA suppresses glioblastoma development in a mechanically sensitive manner. *Proc. Natl. Acad. Sci. USA* **116**, 15550-15559. doi:10.1073/pnas.1902847116

Rahman, M. A., Reuther, C., Lindberg, F. W., Mengoni, M., Salhotra, A., Heldt, G., Linke, H., Diez, S. and Månsson, A. (2019). Regeneration of assembled, molecular-motor-based bionanodevices. *Nano Lett.* **19**, 7155-7163. doi:10.1021/acs.nanolett.9b02738

Reuther, C., Catalano, R., Salhotra, A., Vemula, V., Korten, T., Diez, S. and Månsson, A. (2021a). Comparison of actin- and microtubule-based motility systems for application in functional nanodevices. *New J. Phys.* **23**, 075007. doi:10.1088/1367-2630/ac10ce

Reuther, C., Steenhusen, S., Meinecke, C. R., Surendiran, P., Salhotra, A., Lindberg, F. W., Månsson, A., Linke, H. and Diez, S. (2021b). Molecular motor-driven filament transport across three-dimensional, polymeric micro-junctions. *New J. Phys.* **23**, 125002. doi:10.1088/1367-2630/ac39b4

Ross, J. L., Ali, M. Y. and Warshaw, D. M. (2008). Cargo transport: molecular motors navigate a complex cytoskeleton. *Curr. Opin. Cell Biol.* **20**, 41-47. doi:10.1016/j.ceb.2007.11.006

Sakamoto, T., Wang, F., Schmitz, S., Xu, Y., Xu, Q., Molloy, J. E., Veigel, C. and Sellers, J. R. (2003). Neck length and processivity of myosin V. *J. Biol. Chem.* **278**, 29201-29207. doi:10.1074/jbc.M303662200

Salhotra, A., Zhu, J. Y., Surendiran, P., Meinecke, C. R., Lyttleton, R., Usaj, M., Lindberg, F. W., Norrby, M., Linke, H. and Månsson, A. (2021). Prolonged function and optimization of actomyosin motility for upscaled network-based biocomputation. *New J. Phys.* **23**, 085005. doi:10.1088/1367-2630/ac1809

Saper, G. and Hess, H. (2020). Synthetic systems powered by biological molecular motors. *Chem. Rev.* **120**, 288-309. doi:10.1021/acs.chemrev.9b00249

Stewart, M. A., Franks-Skiba, K., Chen, S. and Cooke, R. (2010). Myosin ATP turnover rate is a mechanism involved in thermogenesis in resting skeletal muscle fibers. *Proc. Natl. Acad. Sci. USA* **107**, 430-435. doi:10.1073/pnas.0909468107

Sundberg, M., Rosengren, J. P., Bunk, R., Lindahl, J., Nicholls, I. A., Tagerud, S., Omling, P., Montelius, L. and Månsson, A. (2003). Silanized surfaces for in vitro studies of actomyosin function and nanotechnology applications. *Anal. Biochem.* **323**, 127-138. doi:10.1016/j.ab.2003.07.022

Sundberg, M., Balaz, M., Bunk, R., Rosengren-Holmberg, J. P., Montelius, L., Nicholls, I. A., Omling, P., Tagerud, S. and Månsson, A. (2006a). Selective spatial localization of actomyosin motor function by chemical surface patterning. *Langmuir* **22**, 7302-7312. doi:10.1021/la060365i

Sundberg, M., Bunk, R., Albet-Torres, N., Kvennefors, A., Persson, F., Montelius, L., Nicholls, I. A., Ghatnekar-Nilsson, S., Omling, P., Tagerud, S. et al. (2006b). Actin filament guidance on a chip: toward high-throughput assays and lab-on-a-chip applications. *Langmuir* **22**, 7286-7295. doi:10.1021/la060854i

Surendiran, P., Meinecke, C. R., Salhotra, A., Heldt, G., Zhu, J., Månsson, A., Diez, S., Reuter, D., Kugler, H., Linke, H. et al. (2022). Solving exact cover instances with molecular-motor-powered network-based biocomputation. *ACS Nanosci. Au.* **2**, 396-403. doi:10.1021/acsnanoscienceau.2c00013

Suzuki, H., Yamada, A., Oiwa, K., Nakayama, H. and Mashiko, S. (1997). Control of actin moving trajectory by patterned poly(methylmethacrylate) tracks. *Biophys. J.* **72**, 1997-2001. doi:10.1016/S0006-3495(97)78844-1

Takatsuki, H., Bengtsson, E. and Månsson, A. (2014). Persistence length of fascin-cross-linked actin filament bundles in solution and the in vitro motility assay. *Biochim. Biophys. Acta Gen. Subj.* **1840**, 1933-1942. doi:10.1016/j.bbagen.2014.01.012

Ten Siethoff, L., Lard, M., Generosi, J., Andersson, H. S., Linke, H. and Månsson, A. (2014). Molecular motor propelled filaments reveal light-guiding in nanowire arrays for enhanced biosensing. *Nano Lett.* **14**, 737-742. doi:10.1021/nl404032k

Toepfer, C. N., Garfinkel, A. C., Venturini, G., Wakimoto, H., Repetti, G., Alamo, L., Sharma, A., Agarwal, R., Ewoldt, J. F., Cloonan, P. et al. (2020). Myosin sequestration regulates sarcomere function, cardiomyocyte energetics, and metabolism, informing the pathogenesis of hypertrophic cardiomyopathy. *Circulation* **141**, 828-842. doi:10.1161/CIRCULATIONAHA.119.042339

Trivedi, D. V., Nag, S., Spudich, A., Ruppel, K. M. and Spudich, J. A. (2020). The myosin family of mechanoenzymes: from mechanisms to therapeutic approaches. *Annu. Rev. Biochem.* **89**, 667-693. doi:10.1146/annurev-biochem-011520-105234

Usaj, M., Moretto, L. and Månsson, A. (2022). Critical evaluation of current hypotheses for the pathogenesis of hypertrophic cardiomyopathy. *Int. J. Mol. Sci.* **23**, 2195. doi:10.3390/ijms23042195

Vahokoski, J., Calder, L. J., Lopez, A. J., Molloy, J. E., Kursula, I. and Rosenthal, P. B. (2022). High-resolution structures of malaria parasite actomyosin and actin filaments. *PLoS Pathog.* **18**, e1010408. doi:10.1371/journal.ppat.1010408

Van Delft, F. C. M. J. M., Månsson, A., Kugler, H., Korten, T., Reuther, C., Zhu, J. Y., Lyttleton, R., Blaudeck, T., Meinecke, C. R., Reuter, D. et al. (2022). Roadmap for network-based biocomputation. *Nano Futures* **6**, 032002. doi:10.1088/2399-1984/ac7d81

Van Den Heuvel, M. G. L. and Dekker, C. (2007). Motor proteins at work for nanotechnology. *Science* **317**, 333-336. doi:10.1126/science.1139570

Van Den Heuvel, M. G., Butcher, C. T., Smeets, R. M., Diez, S. and Dekker, C. (2005). High rectifying efficiencies of microtubule motility on kinesin-coated gold nanostructures. *Nano Lett.* **5**, 1117-1122. doi:10.1021/nl0506554

Van Zalinge, H., Aveyard, J., Hajne, J., Persson, M., Månsson, A. and Nicolau, D. V. (2012). Actin filament motility induced variation of resonance frequency and rigidity of polymer surfaces studied by quartz crystal microbalance. *Langmuir* **28**, 15033-15037. doi:10.1021/la302717y

Van Zalinge, H., Ramsey, L. C., Aveyard, J., Persson, M., Månsson, A. and Nicolau, D. V. (2015). Surface-controlled properties of myosin studied by electric field modulation. *Langmuir* **31**, 8354-8361. doi:10.1021/acs.langmuir.5b01549

Vikhorev, P. G., Vikhoreva, N. N. and Månsson, A. (2008). Bending flexibility of actin filaments during motor-induced sliding. *Biophys. J.* **95**, 5809-5819. doi:10.1529/biophysj.108.140335

Whitesides, G. M. (2006). The origins and the future of microfluidics. *Nature* **442**, 368-373. doi:10.1038/nature05058

Yotti, R., Seidman, C. E. and Seidman, J. G. (2019). Advances in the genetic basis and pathogenesis of sarcomere cardiomyopathies. *Annu. Rev. Genomics Hum. Genet.* **20**, 129-153. doi:10.1146/annurev-genom-083118-015306

Zhu, J. Y., Salhotra, A., Meinecke, C. R., Surendiran, P., Lyttleton, R., Reuter, D., Kugler, H., Diez, S., Månsson, A., Linke, H. et al. (2022). Solving the 3-satisfiability problem using network-based biocomputation. *Adv. Intell. Syst.* **4**, 2200202. doi:10.1002/aisy.202200202